Bioorganic & Medicinal Chemistry Letters 21 (2011) 3237–3242

Contents lists available at ScienceDirect

Bioorganic & Medicinal Chemistry Letters

journal homepage: www.elsevier.com/locate/bmcl

# Orally active aminopyridines as inhibitors of tetrameric fructose-1,6-bisphosphatase

Paul Hebeisen [a], Wolfgang Haap [a], Bernd Kuhn [a], Peter Mohr [a], Hans Peter Wessel [a], Ulrich Zutter [a], Stephan Kirchner [b], Armin Ruf [a], Jörg Benz [a], Catherine Joseph [a], Rubén Alvarez-Sánchez [a], Marcel Gubler [a], Brigitte Schott [a], Agnes Benardeau [a], Effie Tozzo [a], Eric Kitas [a,*]

[a] F. Hoffmann-La Roche Ltd, Discovery Research Basel, CH-4070 Basel, Switzerland
[b] F. Hoffmann-La Roche Ltd, Non Clinical Safety, CH-4070 Basel, Switzerland

ARTICLE INFO

*Article history:*
Received 23 February 2011
Revised 8 April 2011
Accepted 12 April 2011
Available online 20 April 2011

*Keywords:*
Fructose-1,6-bisphosphatase
FBPase
Allosteric inhibition
Structure–activity studies
X-ray crystallography
Genotoxicity
Glucose reduction
db/db Mouse model

ABSTRACT

A novel sulfonylureido pyridine series exemplified by compound **19** yielded potent inhibitors of FBPase showing significant glucose reduction and modest glycogen lowering in the acute db/db mouse model for Type-2 diabetes. Our inhibitors occupy the allosteric binding site and also extend into the dyad interface region of tetrameric FBPase.



Targeting fructose-1,6-bisphosphatase (FBPase) is a potentially viable approach for glucose control in Type-2 diabetes (T2D). Numerous publications have recently appeared describing FBPase inhibitors[1] and, furthermore, molecules from Metabasis Inc. have been advanced to human clinical trials.[2] Besides its role in gluconeogenesis control, FBPase has also been implicated in glucose sensing and in regulating insulin secretion in β-cells.[3] We have previously described our aminothiazole class of small molecule inhibitors of FBPase which were shown to significantly lower fasting glucose levels in a transgenic mouse model of T2D.[4] During the optimization phase we investigated the liability of advanced molecules to be oxidized to thioureas which have been associated with lipidosis. Although, we concluded that the very low level of thiourea metabolite measured in this study not to be a potential risk, we also identified six-membered (hetero)aromatic bioisosteres of aminothiazoles as potent FBPase inhibitors, which are the subject of this paper.

As previously outlined, our series occupy the allosteric AMP binding site and reach through the sulfonylureido linker into a second binding region, at the dyad interface of tetrameric FBPase.[4] In the interface region, there are direct π-stacking interactions between the terminal thiazole rings of two adjacent ligands as well as several strong van der Waals interactions between highly polarizable ligand substituents, such as –Br, –SMe, or –Cl and the side chains of Met18A/C (Fig. 1, left panel). Activity in the thiazole series could be increased by up to a factor of 80 by these specific substitutions. In this paper, we will focus on the replacement of the aminothiazole motif while trying to satisfy the main recognition motifs (π-stacking of aromatic ring, polarizable substituent close to Met18) and discuss the evolving SAR.[5] The structure–activity relationship of the (hetero)aromatic sulfonylureido moiety occupying the AMP binding site paralleled that of the aminothiazole series and could be transferred to a considerable extent to the new series reported here. We mainly use 3-Cl substituted phenyl and 5-(2-methoxy-ethyl)-4-methyl substituted thiophenyl (Table 1), which have been identified as high affinity fragments in our previous publication.[4] While both *meta*-Cl in the phenyl and β-methyl in the thiophene series occupy the back pocket in the AMP binding site, the methoxyethyl substituent in the α-position of the thiophene ring makes additional non-polar interactions with Leu30 and Val160 of human liver FBPase (X-ray structure not shown) further enhancing the binding affinity in this series.

* Corresponding author. Tel.: +41 61 6887618; fax: +41 61 6886459.
*E-mail address:* eric_a.kitas@roche.com (E. Kitas).

0960-894X/$ - see front matter © 2011 Elsevier Ltd. All rights reserved.
doi:10.1016/j.bmcl.2011.04.044

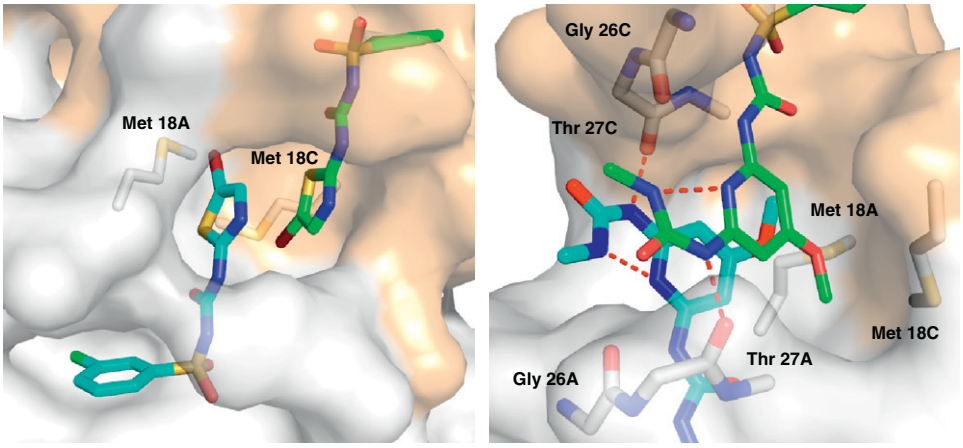


**Figure 1.** Left: X-ray structure of human liver FBPase with compound **1** (cyan). The *meta*-chlorophenyl ring occupies the AMP binding region while the bromothiazole moiety is involved in interactions at the dyad interface, including contacts to a neighboring ligand (green). Solvent-accessible surfaces of the two protein chains A and C are colored white and gold, respectively. Right: X-ray structure of FBPase dyad interface region in complex with two ligands **10** (cyan, green). Hydrogen bonds of the urea-substituted pyridines are depicted with red, dashed lines.[6]

**Table 1**
FBPase inhibition: N-heterocycle analogues[a]

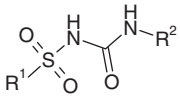

| Entry | $R^1$ | $R^2$ | HL $IC_{50}$ (μM) | ML $IC_{50}$ (μM) | $mEC_{50}$ (μM) |
|---|---|---|---|---|---|
| **1** |  | 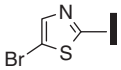 | 0.33 | 5.79 | 49 |
| **2** |  | 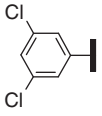 | 0.64 | 12 | 84 |
| **3** |  | 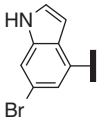 | 0.35 | 5.0 | 41 |
| **4** |  | 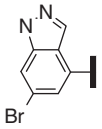 | 0.33 | 3.3 | 23 |
| **5** |  | 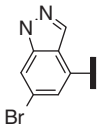 | 0.29 | 4.5 | 13 |
| **6** | 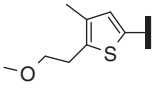 | 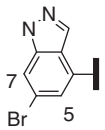 | 0.14 | 1.7 | 6.1 |
| **7** | 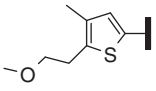 | 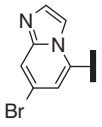 | 0.82 | 8 | 51 |

**Table 1** (*continued*)

| Entry | $R^1$ | $R^2$ | HL $IC_{50}$ (μM) | ML $IC_{50}$ (μM) | $mEC_{50}$ (μM) |
|---|---|---|---|---|---|
| **8** | 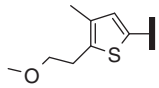 | 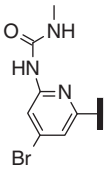 | 0.08 | 1.0 | 5 |
| **9** | 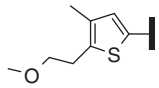 | 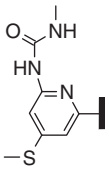 | 0.17 | 1.6 | 8 |
| **10** | 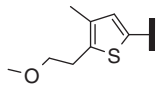 | 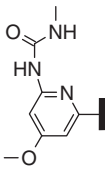 | 0.22 | 2.6 | 12 |
| **11** | 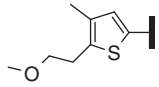 | 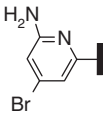 | 0.13 | 1.5 | 8 |
| **12** | 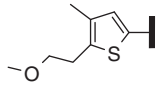 | 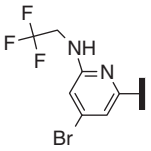 | 0.20 | 3.7 | 14 |
| **13** | 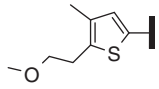 | 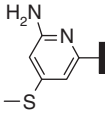 | 1.8 | 9 | 7 |
| **14** | 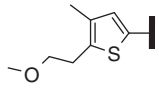 | 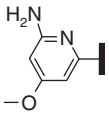 | 0.4 | 30 | 97 |
| **15** | 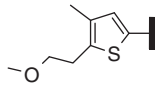 | 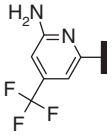 | 0.76 | 6 | 8 |
| **16** | 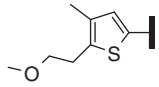 | 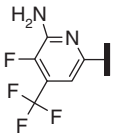 | 0.60 | 3.5 | 8.9 |
| **17** | 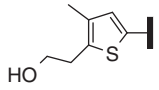 | 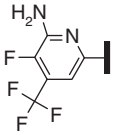 | 0.42 | 4 | 4 |
| **18** | 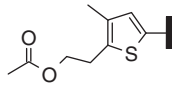 | 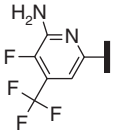 | 0.67 | 3.5 | 2.7 |
| **19** | 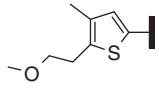 | 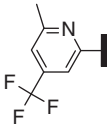 | 0.53 | 7 | 5.9 |

(*continued on next page*)

**Table 1** (*continued*)

| Entry | $R^1$ | $R^2$ | HL $IC_{50}$ (μM) | ML $IC_{50}$ (μM) | $mEC_{50}$ (μM) |
|---|---|---|---|---|---|
| **20** | 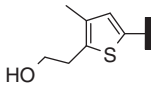 | 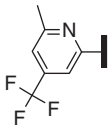 | 0.35 | 4 | 8.3 |
| **21** | 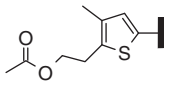 | 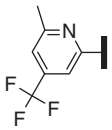 | 0.52 | 7.3 | 5.1 |
| **22** | 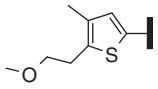 | 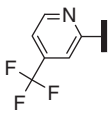 | 1.7 | 8.3 | 19 |

[a] HL $IC_{50}$ and ML $IC_{50}$ values represent potency of FBPase inhibitors against human liver and mouse liver FBPase, respectively, as determined in enzyme inhibition assays described previously.[9] $mEC_{50}$ values are a measure of efficacy of FBPase inhibitors in cultivated primary mouse hepatocytes to suppress glucose production.[10]

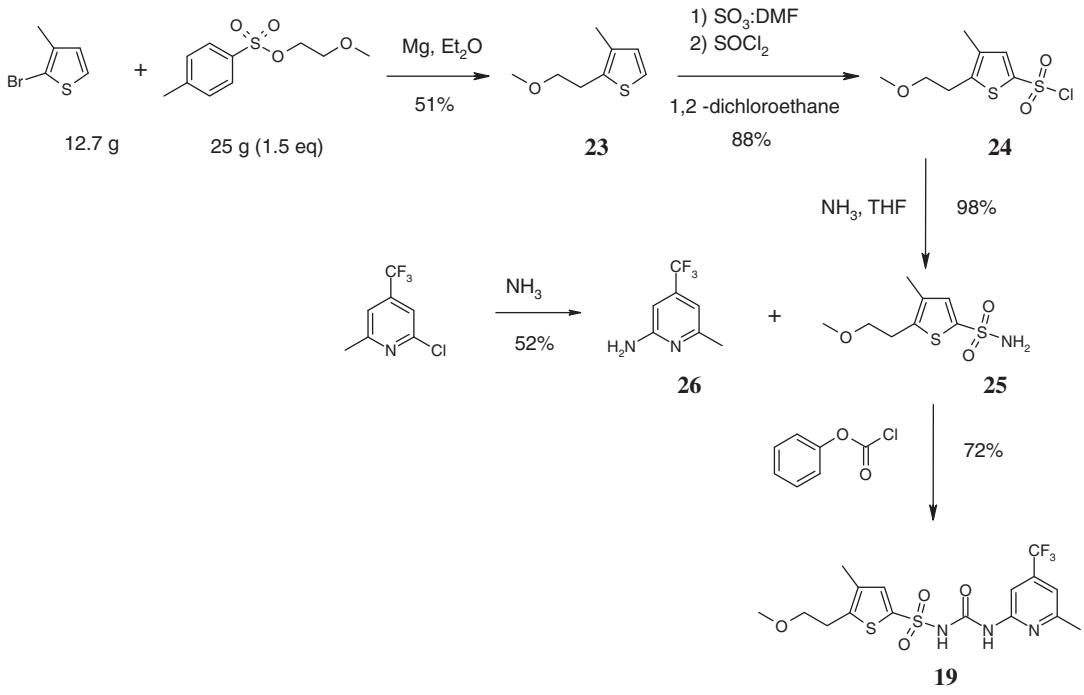


**Scheme 1.** Outlining sulfonamide approach for the preparation of FBPase inhibitor **19**.

The dichlorophenyl analog **2** was a first example of a thiazole replacement with modest enzymatic activity against both human and mouse isoforms of FBPase although exhibiting poor efficacy in the mouse hepatocyte assay (Table 1). Due to the strong, positive impact of –Br substitution on FBPase binding, we performed a virtual screen of available building blocks that would position the Br atom close to the Met18 side chains. From this exercise, 6-Br-substituted indoles and subsequently indazoles could be identified. Compound **6** showed both impressive activities in the enzymatic as well as the cellular assay, with a mouse $EC_{50}$ of 6.1 μM. As part of the multi-dimensional optimization process, compounds were routinely submitted to safety assays such as the AMES test for genotoxicity where positive results were obtained for FBPase inhibitors bearing the indazole moiety.[7] Typically, a greater than two-fold induction of mutant colonies was found in the TA98 strain after metabolic activation. Blocking the vulnerable 5-position on the indazole ring with Cl reduced the AMES activity but abolished FBPase inhibition as well. Replacing the indazole by imidazopyridine **7** removed the AMES activity but yielded also only modest inhibition of the enzyme.

With the help of molecular modeling and searches in the small molecule X-ray Cambridge Structural Database[8] we identified urea-substituted pyridines as potential bioisosteres of indazoles. These replacements (Table 1, compounds **8–10**) were well tolerated provided that the terminal nitrogen atom carried at least one hydrogen atom. The hypothesis that, in the binding conformation, this hydrogen atom was involved in an intramolecular hydrogen bond was nicely confirmed by X-ray crystallography (Fig. 1, right panel). The crystal structure further revealed a hydrogen bond between the proximal nitrogen atom of the urea substituent with the O=C backbone of Thr27 from a neighboring subunit (ligand A with Thr27C and ligand C with Thr27A, respectively), and

**Table 2**
ADME profile and mouse PK/PD parameters of selected aminopyridines

| FBPase inhibitors | **16** | **18** | **19** | **20** | **21** |
|---|---|---|---|---|---|
| Mouse $EC_{50}$ (μM) | 8.9 | 2.7 | 5.9 | 8.3 | 5.1 |
| Cl(human)[a] (μl/min/mg protein) | 10.0 | Unstable | nd | 28 | Unstable |
| Cl (mice)[a] (μl/min/mg protein) | 12.1 | Unstable | 31 | 10 | Unstable |
| Solubility (mg/mL) | 0.53 | 0.16 | >0.49 | >0.57 | >0.62 |
| PAMPA[b] Pe ($\times 10^{-6}$/s) | 4.0 | nd[c] | 1.7 | 0.7 | 1.4 |
| Plasma levels at 6 h (ng/mL) | 4091 | nd | 2794 | 6799 | nd |
| Liver-to-plasma ratio | 17.4 | nd | 10.5 | 8.9 | nd |
| Glucose reduction after 6 h[d] (%) | 31[f] | 16[e] | 38[f] | 36[f] | 29[f] |
| Liver glycogen reduction after 6 h (%) | 18 | Increased by 21 | 33[f] | 8 | 5 |

[a] Microsomal intrinsic clearance.
[b] PAMPA is a prediction assay for oral absorption.[13]
[c] nd = not determined measurement.
[d] Acute glucose lowering in db/db mouse model [dose = 100 mg/kg po].
[e] Acute glucose lowering in db/db mouse model [dose = 200 mg/kg po].
[f] Significantly different from vehicle ($p$ <0.05).

nicely illustrates the planarity of the urea-substituted pyridine resulting in extended π-stacking of both heterocycles. Thus, despite having formally two more hydrogen-bonding groups, the ureido analog **8** acts as a bioisostere of the bicyclic indazole **6**.

Simplifying the structure to the aminopyridine **11** maintained strong FBPase inhibition but induced again AMES activity. Amine alkylation however, as in **12**, fixed this flaw. The mutagenicity potential was also consistently overcome when 4-Br replacements were identified such as thiomethoxy in **13**, methoxy- in **14** and the $CF_3$ group in compound **15**. The 4-trifluoromethyl aminopyridines were further pursued and gave efficacious compounds not requiring the amine functionality such as **19** and **20**. The esterase labile acetates **18** and **21** were prepared to explore the potential modulation of pharmacokinetic properties of the parent alcohols **17** and **20**, respectively. Interestingly, no significant loss of in vitro efficacy was observed following this transformation.

Our general and straightforward synthetic approach to the aminopyridine series can be exemplified with the $CF_3$-substituted derivative **19** (Scheme 1). 2-Bromo-3-methyl-thiophene was transformed to the corresponding Grignard reagent which was treated with toluene-4-sulfonic acid 2-methoxyl ethyl ester affording compound **23** in a modest 51% yield. Formation of the sulfonyl chloride **24** using the DMF–sulfur trioxide complex followed by chlorination of the resultant sulfonate with thionyl chloride was achieved in an overall 88% yield. Ammonolysis yielded sulfonamide **25** which was finally coupled to the phenyl-carbamate derivative of 6-methyl-4-trifluoromethyl-pyridin-2-ylamine **26** using triethylamine as base.

A series of 4-trifluoromethyl aminopyridines with promising properties (high aqueous solubility and *PAMPA* permeability) and good efficacy in primary hepatocytes were further profiled in the acute, db/db mouse model for T2D.[11] Compounds were p.o. administered (100 mg/kg or 200 mg/kg) to 15 week-old db/db mice 4 h after food removal (in the morning). Surprisingly and in contrast to our previously described aminothiazole series, aminopyridines **16**, **19**, and **20** that were in vivo tested showed high liver partitioning. Furthermore, all the selected FBPase inhibitors **16**, **19–21**, except **18**, decreased significantly blood glucose levels in comparison to vehicle at 6 h post-dosing (overall, reduction reached 29–38% compared to vehicle, $p$ <0.05, see Table 2).[12] Liver glycogen was significantly decreased after treatment with compound **19**.

Looking at derisking the potential for toxic metabolite formation from our original aminothiazole FBPase inhibitor series, we proceeded to successfully identify N-heterocycle isosteres that maintained strong in vitro activity against this important enzyme in the gluconeogenesis pathway. Furthermore, robust glucose reduction in an acute mouse model for T2D was demonstrated with a set of $CF_3$-substituted aminopyridines.

## Acknowledgements

The excellent technical assistance of Betty Hennequin, Patrick Studer, Lilli Anselm, Stefan Thomi, Tamara Codilupi, Annie Sellam, Edith Brandt, Raymonde Schmitt, Anthony Vandjour and Stefan Masur is gratefully acknowledged.

## References and notes

1. Dang, Q.; Kasibhatla, S. R.; Xiao, W.; Liu, Y.; Da Re, J.; Taplin, F.; Reddy, K. R.; Scarlato, G. R.; Gibson, T.; van Poelje, P. D.; Potter, S. C.; Erion, M. D. *J. Med. Chem.* **2010**, *53*, 441; Tsukada, T.; Kanno, O.; Yamane, T.; Tanaka, J.; Yoshida, T.; Okuno, A.; Shiiki, T.; Takahashi, M.; Nishi, T. *Bioorg. Med. Chem.* **2010**, *18*, 5346; Rudnitskaya, A.; Borkin, D. A.; Huynh, K.; Torok, B.; Stieglitz, K. *ChemMedChem* **2010**, *5*, 384; Heng, S.; Gryncel, K. R.; Kantrowitz, E. R. *Bioorg. Med. Chem.* **2009**, *17*, 3916.
2. Dang, Q.; Liu, Y.; Cashion, D. K.; Kasibhatla, S. R.; Jiang, T.; Taplin, F.; Jacintho, J. D.; Li, H.; Sun, Z.; Fan, Y.; DaRe, J.; Tian, F.; Li, W.; Gibson, T.; Lemus, R.; van Poelje, P. D.; Potter, S. C.; Erion, M. D. *J. Med. Chem.* **2011**, *54*, 153.
3. Zhang, Y.; Xie, Z.; Zhou, G.; Zhang, H.; Lu, J.; Zhang, W. J. *Endocrinology* **2010**, *151*, 4688.
4. Kitas, E.; Mohr, P.; Kuhn, B.; Hebeisen, P.; Wessel, H. P.; Haap, W.; Ruf, A.; Benz, J.; Joseph, C.; Huber, W.; Sanchez, R. A.; Paehler, A.; Benardeau, A.; Gubler, M.; Schott, B.; Tozzo, E. *Bioorg. Med. Chem. Lett.* **2010**, *20*, 594.
5. Structure–activity relationship (SAR) was built using $IC_{50}$ data of the human and mouse liver enzymes. Efficacy data on mouse hepatocytes were collected in parallel and used for selecting compounds for subsequent in vivo experiments in mouse models.
6. Crystallographic data were collected on beam line X10SA at the Swiss Light Source and coordinates were deposited with the PDB-codes 2y5l and 2y5k for compounds **1** and **10**, respectively.
7. Genotoxicity is estimated with the use of the AMES microsuspension assay, where the readout parameter is the increase in the number of revertant colonies (mutation frequency) of treated compared to untreated control in five different *Salmonella triphimurium* tester strains.
8. Allen, F. *Acta Crystallogr., Sect. B* **2002**, *58*, 380.
9. Hebeisen, P.; Kuhn, B.; Kohler, P.; Gubler, M.; Huber, W.; Kitas, E.; Schott, B.; Benz, J.; Joseph, C.; Ruf, A. *Bioorg. Med. Chem. Lett.* **2008**, *18*, 4708.
10. Primary mouse hepatocytes were seeded in 96-well tissue culture plates (25,000 cells per well) in 100 μl of DMEM medium (Invitrogen) containing 10% fetal bovine serum (FBS). After 24 h of cultivation at 37 °C, the medium was replaced with 100 μl of RPMI medium without glucose (Invitrogen) containing 1% FBS. The cells were incubated for 24 h at 37 °C for starvation and depletion of intracellular glycogen. After removal of medium and washing with phosphate-buffered saline (PBS, Invitrogen), the cells were incubated with FBPase inhibitors for 6 h at 37 °C in 60 μl of PBS containing 0.1% bovine serum albumin (BSA), 20 mM lactate and 2 mM pyruvate. Glucose produced and released by the cells was determined in the culture supernatant using the glucose oxidase assay (Amplex Red kit, Molecular Probes).
11. Fifteen week-old male db/db mice on C57BLKS background were kept under controlled-fed-conditions and then block randomized based on blood glucose levels. Bodyweight was measured in the morning 4 h after food removal (postprandial conditions) and the mice were then immediately orally dosed with 4 mL/kg vehicle (0.5% Tween 80, 0.5% hydroxyethylcellulose) (0.3% Tween 80) or FBPase inhibitors at 100 mg/kg or 200 mg/kg. The FBPase inhibitor CS-917 was used as the positive control.[2] Blood glucose was monitored with a hand held glucose monitoring device (AccuCheck, Roche Diagnostics) at times 0, +2, +4 and +6 h post dose by tail tip bleed. Full blood ($N$ = 8 per group) was collected (on EDTA). After the last blood glucose measurement, mice were sacrificed by decapitation immediately after the 6 h time-point and blood and

liver were collected for determining compound exposure and liver glycogen analysis. Glucose (Glc) results are expressed as % lowering versus the vehicle group at the same time-point. Glucose data were analyzed using the software JMP6 for Windows (Version 5.01, SAS institute Inc., SAS Campus Drive, Cary, NC 27513). Analysis of Variance ANOVA (alpha 0.05 and 0.01) followed by Dunnett's test (comparison vs control).

12. Animals were randomized according to body weight and glucose level measured at baseline before compounds administration. Livers were of normal appearance (normal color, no hypertrophy, no increase in weight compared to vehicle-treated mice).
13. Kansy, M.; Fischer, H.; Kratzat, K.; Senner, F.; Wagner, B.; Parrilla, I. *Helv. Chim. Acta* **2000**, 447.

| | | Glc (mM) 0 h | Glc (mM) +2 h | Glc (mM) +4 h | Glc (mM) +6 h |
|---|---|---|---|---|---|
| **Vehicle** | Mean | 22.73 | 31.16 | 26.58 | 23.84 |
| | SEM | 0.73 | 0.63 | 1.09 | 0.98 |
| **16** (100 mg/kg) | Mean | 22.49 | 26.99 | 19.04 | 16.24 |
| | SEM | 0.75 | 1.78 | 1.41 | 1.70 |
| Compd **16** versus vehicle (%) | | | | | −31 |
| **18** (200 mg/kg) | Mean | 22.46 | 27.59 | 23.31 | 20.09 |
| | SEM | 0.72 | 1.29 | 0.75 | 0.90 |
| Compd **18** versus vehicle (%) | | | | | −16 |
| **19** (100 mg/kg) | Mean | 22.55 | 21.91 | 16.60 | 14.64 |
| | SEM | 0.85 | 1.24 | 1.35 | 1.42 |
| Compd **19** versus vehicle (%) | | | | | −38 |
| **20** (100 mg/kg) | Mean | 22.53 | 23.68 | 18.86 | 16.79 |
| | SEM | 0.77 | 1.10 | 1.54 | 1.47 |
| Compd **20** versus vehicle (%) | | | | | −36 |
| **21** (100 mg/kg) | Mean | 22.48 | 24.66 | 18.76 | 14.95 |
| | SEM | 0.79 | 0.80 | 1.26 | 0.86 |
| Compd **21** versus vehicle (%) | | | | | −29 |
| **CS-917** (200 mg/kg) | Mean | 22.69 | 29.59 | 21.25 | 18.61 |
| | SEM | 0.76 | 1.61 | 1.32 | 1.73 |
| **CS-917** versus vehicle (%) | | | | | −22 |